Heliyon 10 (2024) e26395

Contents lists available at ScienceDirect

Heliyon

journal homepage: www.cell.com/heliyon

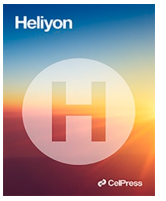

Research article

Adaptive neuro-fuzzy inference system for forecasting corrosion rates of automotive parts in biodiesel environment

Olusegun David Samuel [a,b,*], Modestus O. Okwu [a], Varatharajulu M [c], Ivrogbo Daniel Eseoghene [a], H. Fayaz [d]

[a] Department of Mechanical Engineering, Federal University of Petroleum Resources, Effurun, Delta State P.M.B 1221, Nigeria
[b] Department of Mechanical Engineering, University of South Africa, Science Campus, Private Bag X6, Florida, 1709, South Africa
[c] Sri Krishna College of Technology, Kovaipudur, Coimbatore, Tamil Nadu 641 042, India
[d] Modeling Evolutionary Algorithms Simulation and Artificial Intelligence, Faculty of Electrical and Electronics Engineering, Ton Duc Thang University, Ho Chi Minh City, Vietnam

ARTICLE INFO

Keywords:
Response surface methodology (RSM)
Adaptive neuro-fuzzy inference (ANFIS)
Corrosion
Copper
Brass
Biodiesel

ABSTRACT

It is precarious to scrutinize the impacts of operational parameters on corrosion when choosing materials for the green diesel and automotive industries. This was the original study to showcase an optimization stratagem for abating corrosion rates (CRs) of automotive parts (APs) explicitly copper and brass in a biodiesel environment, adopting novel Response Surface Methodology (RSM) and Adaptive Neuro-Fuzzy Inference System (ANFIS).To model CRs, the RSM and ANFIS were utilized. The mechanical properties of APs were inspected, explicitly their hardness number and tensile strength, as well as their outward morphologies. The optimal CRs for copper and brass were 0.01656 mpy and 0.008189 mpy at a B 3.91 biodiesel/diesel blend and 240.9-h exposure. The ANFIS model had a higher coefficient of determination and lower values of root mean squared errors (RMSE), mean average error (MAE), and average absolute deviation (AAD) when compared to the RSM model; this authenticates the ANFIS model's superiority for predicting CRs of copper and brass. The tensile strength of brass was greater than that of copper, while the latter had a higher hardness number. The information, model, and correlations can assist APS in mitigating and slaving over for the corrosiveness of APs while utilizing green diesel.

1. Introduction

Given the imminent depletion of fossil resources and the impending threat of an energy crisis, it is vital to advance emerging solutions to address both existing and future energy hardships [1]. Biodiesel is an excellent diesel fuel alternative because of its minimal environmental impact, biodegradability, and convenience to combat global warming [2]. Transesterification is used for the production of biodiesel, a more environmentally friendly substitute to diesel fuel [3]. The dose and kind of catalyst used, the molar ratio, the temperature, and the time essential to produce the ester are all factors that affect (m)ethyl yield [4]. Owing to its enhanced cetane number, superior lubricity, lesser sulfur content, and advanced flash point, biodiesel has outperformed fossil fuels in admiration [5]. It has unwanted poor cold flow features, advanced viscosity, and volatility, and is more predisposed to corrosion or degradation of

* Corresponding author. Department of Mechanical Engineering, Federal University of Petroleum Resources, Effurun, Delta State P.M.B 1221, Nigeria.
E-mail address: samuel.david@fupre.edu.ng (O.D. Samuel).

https://doi.org/10.1016/j.heliyon.2024.e26395
Received 6 March 2023; Received in revised form 12 February 2024; Accepted 12 February 2024
Available online 19 February 2024

APs [2]. The corrosive nature of automotive parts is triggered of by a lack of compatibility with other APs [5]. The incompatibility is ascribed to copious features such as hygroscopic flora of biodiesel and biodiesel oxidation temperature, moisture content, and microbial stage [2]. The incompatibility is attributed to a variety of factors, including biodiesel hygroscopic flora and biodiesel oxidation temperature, water content, and microbial advancement [6].When an engine component is in promixty with fuel, it is prone to corrosion, initiating the fuel to deteriorate and depart even further from its stipulations [7]. In biodiesel vehicles, for instance, the utilization of copper-based gaskets, washers, and bushings, as well as brass radiator tubes, cores, and tanks, has been constrained [8]. Contemporary discoveries on the corrosion of automotive parts uncovered to green diesel developed from palm oil, Pongamia pinnata oil, Jatropha oil, and Schinzochytrium sp. microalgae have been published [9–12]. However, other researchers [13–15] adopted various tools viz. Taguchi, intelligent technique, RSM for optimizing alga-based bi-hdrogen, valorisation of food waste, water hyacinth operated IC engine, respectively.

It is germane for precise forecasting and monitoring of engine-part durability to have a consistent prediction of the corrosive characteristics of automotive parts exposed to the biodiesel field. Emembolu et al. [16] investigated the prognostic competencies of the RSM and ANFIS models of Al and mild steel corrosion inhibition by Aspilia Africana. Their results indicated the superiority of the ANFIS over RSM technique.

Despite the reality that the fundamental mathematical principles of the process are obscure. Samuel and Okwu [17] indicated that these computational tools provide a way to correlate non-linear information by establishing a link between the system's inputs and outputs. Among the hybrid tools, RSM combined with ANFIS is one that is substantially considered.

The ANFIS model's ability to capture nonlinear structure, adaptability, and rapid learning capacity, combined with usefulness in correlating input vs. response, establishing predictive equations, and inherent optimal conditions in RSM, have made the hybrid model applicable in a wide range of engineering and scientific application fields.

1.1. Motivations, aim and novelty of the study

Table 1 recapitulates the concise review of the numerous model tools espoused to predict metal corrosion rates. Even though many attempts have been made to model and forecast CRs of different metals in various media using different model tools, only Shehzad et al. [18] employed RSM to predict CRs of metals in fat chicken. There hasn't been any earlier study on the RSM and ANFIS-based modelling of CRs of waste-based biodiesel, as far as the authors are aware. To diminish the corrosiveness of APs in biodiesel and fill the knowledge void in the literature, the subsequent actions were implemented: (i) using the Design of Experiments to examine the simultaneous effects of fuel types (0%, 10%, and 10%) and exposure times (240, 480, and 720 hours) on the (CRs) of copper and brass; (ii) investigating into the synergistic effects of corrosion variables; (iii) conducting a study on the interactions between corrosion variables; and (iv) evaluating the efficacy of the RSM and ANFIS of corrosiveness of automotivate parts in green diesel.

The peculiarity of this research lies in the fact that no previous study has evaluated the corrosion rates of Cu and Br exposed to green diesel using RSM-ANFIS methods. Despite such, a variety of research using the RSM and ANFIS techniques to evaluate the corrosion of APs exposed to a biodiesel environment have been published in literary works. The suggested work is undoubtedly novel since there hasn't been much research on the application of the unified RSM-ANFIS approach, tensile strength, and hardness of degraded automotive components, as well as the surface morphology of coupons before and after exposure to a green diesel environment.

The assessments of the hybrid vehicles will demonstrate the efficiency of these fuels, their corrosivity, and their stability in a fuel-metal system, approving the definition of the operating requirements necessary for the practical use of copper and brass in the automotive industry.

Table 1
Review of model tools for corrosion of metals in various media.

Metals	Corrosion media	Model tools	Remarks	References
mild steel and aluminium metal	A. Africana in acid solutions	RSM and ANFIS techniques	ANFIS outperformed RSM technique	Emembolu et al. [16]
Mild steel specimens	micro-/nano-hydroxyapatite (HA) powders	MLs: ANN, RF, SVM, and KNNs	Superiority of RF techniques over other MLs	Aghaaminiha et al. [19]
Ni–Cr–Mo–V	Simulated deep sea environments	DoE and ANN	DoE model exhibited good validity and precision.	Hu et al. [20]
AA6061-T4 alloy coated		ANFIS	Industrial applications of biomedical implant showcased by ANFIS	Tuntas and Dikici [21]
Copper	acid extract of Gnetum Africana (GA)	Factorial DoE (FDoE)	Established suitability of FDoE for optimum GA for reducing corrosion	Nkuzinna et al. [22]
Cu	high-content polyphosphate inhibition	RSM	Efficacy of the RSM established in corrosion minimization of Cu	Goh et al. [23]

MLs = Machine learnhngs, ANN= Artificial neural networks, RF = random forest, SVM = support.
vector machine (SVM), and KNNs = nearest neighbors.

2. Experimental methodology

2.1. Experimental procedure

The splash method was utilized to prepare 10% (B10), 20% (B20), and pure diesel WFOB-diesel blends. The mixtures were thoroughly mixed for 7 min using a magnetic stirrer; no heating was administered. Fig. 1 shows the schematic diagram of the types of fuels. Appendix 1 (Figure A1) depicts the dimension of the vessel employed for keeping fuel types. The fuel kinds were subjected to an ASTM standard regulatory appraisal (see Fig. 2).

Brass and copper bars were used to make experiment coupons. Fig, 2 (a–b) shows the copper and brass coupons' sizes, and Fig, 2(c) shows their respective coupons' chemical compositions. Appendix 2 (Fig. A2) depicts the dimension of apparatus adopted in corrosion testing. The coupons were degreased, polished, immersed in acetone for 30 min, weighed, and then kept in desiccators to avoid air deterioration. The produced coupons were then statically immersed, as reported by Aquino et al. [24] (See Fig. 3a and b). Aquino et al. (2012) investigated the CRs of brass and copper at a temperature of 55 °C. The approach used is compliant with ASTM G1 and ASTM G31 regulations [25]. Computation of the CRs of copper and brass in response to various fuel sources were made using Eqs. (1) and (2). Pre-exposure and post-exposure measurements of thermophysical fuel types were analyzed. Details of the accuracy of equipment utilized are discussed elsewhere [2].

$$CR_{Cu} = \frac{W_{Cu}\ x\ 534}{D_{Cu}A_{Cu}T_{Cu}} \tag{1}$$

$$CR_{Br} = \frac{W_{Br}\ x\ 534}{D_{Br}A_{Br}T_{Br}} \tag{2}$$

where CR_{Cu}, CR_{Br} are the CRs of the copper and brass, W_{Cu} , W_{Br} are the weight losses in copper and copper (mg): the difference between weight prior immersion and weight afterward immersion, D_{Cu}, D_{Br} are the densities of copper and brass (g/cm^3), and T_{Cu}, T_{Br} is the exposure duration of copper and brass to WFOB (hours), respectively.

2.2. Uncertainty analysis of corrosiveness of automotive parts

There are a variety of operational and static immersion tests on gasoline, as well as corrosion studies on automobile elements, which creates some uncertainty. For the time being, guaranteeing the correctness of the experimental setup necessitates an uncertainty evaluation of the precision of the experimentation in conjunction with repeatability.

Table 2 summarizes the uncertainty of all measurements. As discovered, the valuation of critical parameters is presented. The measuring equipment's uncertainty analysis was carried out using the standard technique described elsewhere [26]. The experiment's overall uncertainty analysis was determined using Eq (3). Table 2 summarizes the uncertainty of all measurements.

$$\begin{aligned}\text{Total uncertainity} = \text{Square root of } \Big\{&(\text{uncertainity of exposure duration of Cu/Br})^2 + (\text{uncertainity of weight loss by Cu})^2 \\ &+ (\text{uncerainity of weight loss by Br})^2\Big\}\end{aligned} \tag{3}$$

$$\text{Aggregate uncertainity} = \text{Square root of } \{(0.707107)^2 + (0.003514)^2 + (1.93431)^2\} = \text{Overall uncertainty} = 1.63\ \%;\ \text{i.e. within the range}$$

Fig. 1. Fuel types prepared for corrosion analysis:(a) B0, (b) B10, and (c) B20.

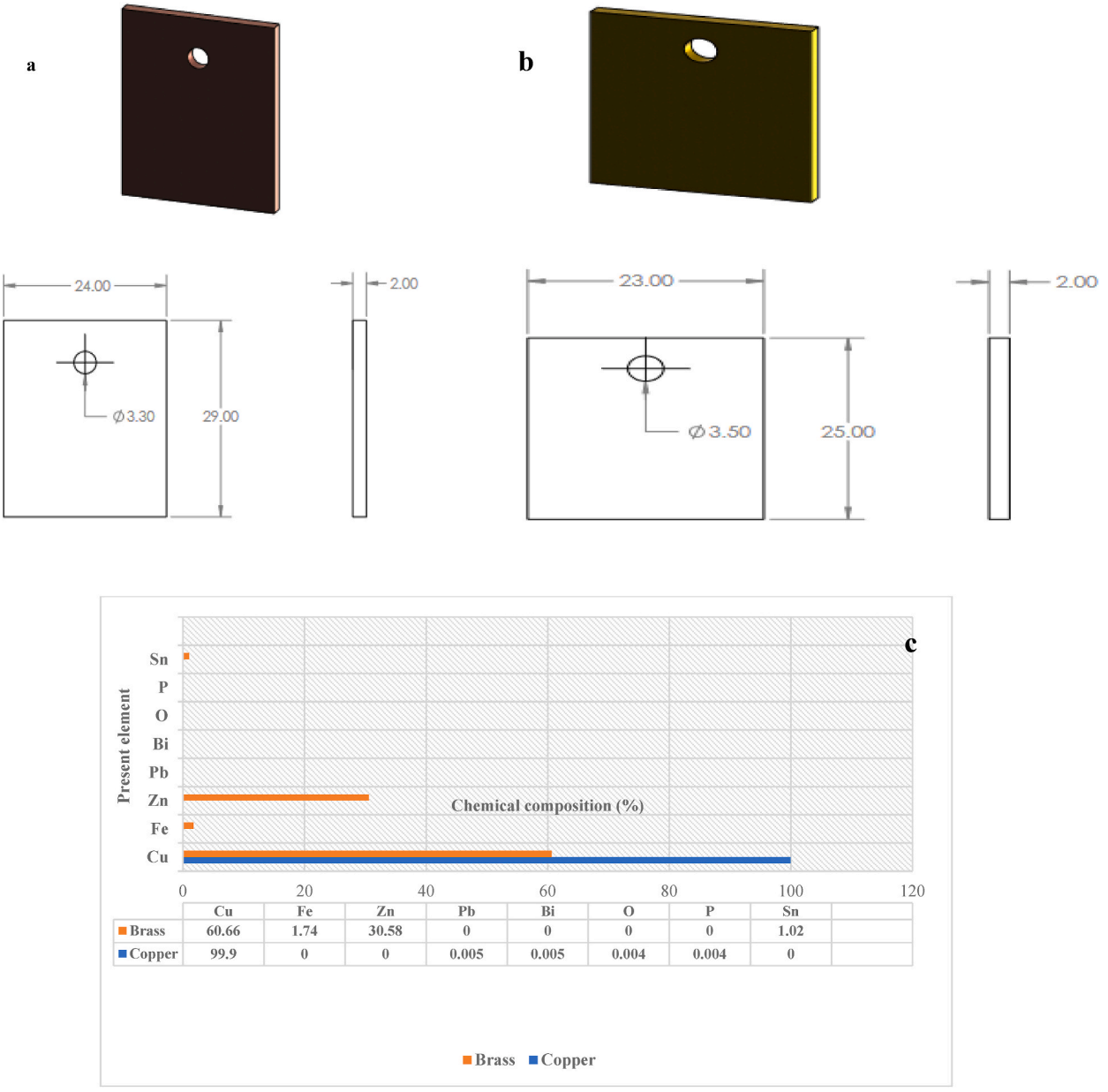

	Cu	Fe	Zn	Pb	Bi	O	P	Sn
Brass	60.66	1.74	30.58	0	0	0	0	1.02
Copper	99.9	0	0	0.005	0.005	0.004	0.004	0

Fig. 2. Specification and dimensions for (a) Br, (b) Cu coupons, and (c) chemical composition.

2.3. Measurement of BHN and TES of degraded Cu and Br

The Brinell hardness number (BRHN) of degraded Cu and Br exposed to various fuel types under optimal conditions was checked using ASTM standard E10-17. The % BRHN was calculated by averaging the results of three successive rounds of tests using Eq. (4).

$$\%\Delta\mathrm{BRHN} = 100 \times \left|\frac{\mathrm{BRHN}_{AE2} - \mathrm{BRHN}_{BE1}}{\mathrm{BRHN}_{BE1}}\right| \tag{4}$$

Corroded coupons were tested for tensile strength (TES, MPa) and percent variation using Eqs. (5) and (6), respectively.

$$\mathrm{TES} = \frac{3,4}{10}\mathrm{BRHN} \tag{5}$$

$$\%\Delta\mathrm{TES} = 100 \times \left|\frac{\mathrm{TES}_{AE2} - \mathrm{TES}_{BE1}}{\mathrm{TES}_{BE1}}\right| \tag{6}$$

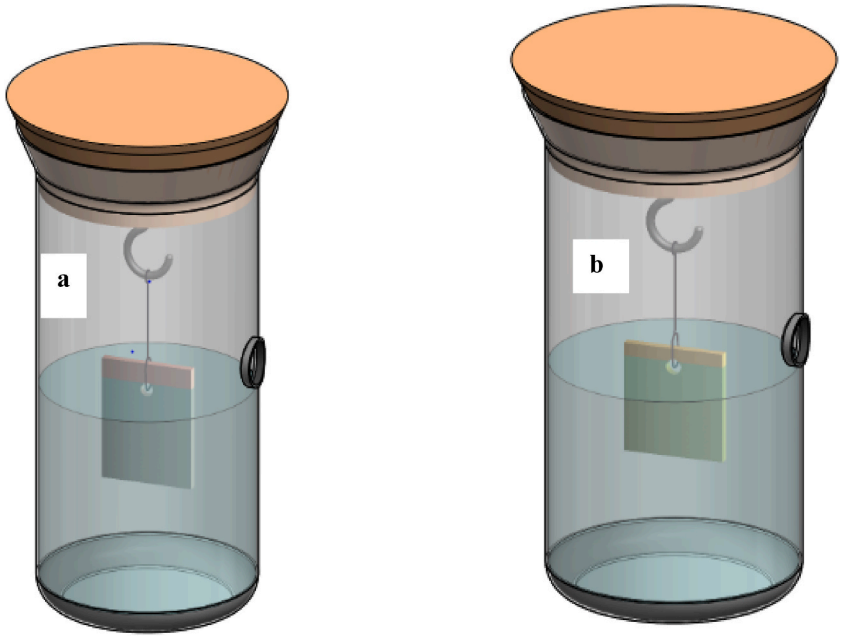

Fig. 3. Schematic for immersion of corrosion testing of coupons: (a) Cu and (b) Br.

Table 2
Uncertainty assessment of corrosion test of automotive parts.

S/N	Computing instruments	Uncertainty
1.	uncertainity of exposure duration of Cu/Br	0.7071
2.	uncertainity of weight loss by Cu	0.003514
3.	uncerainity of weight loss by Br	1.93431

The morphology of the coupons (brass and copper) immersed in the fuel types was inspected using a JCM 100 small scanning electron microscope (Joel, USA).

2.4. Model techniques

2.4.1. Corrosion study via RSM

This experiment used the Central Composite Design (CCD) component of the Response Surface Methodology (RSM). The CRs of copper and brass exposed to different fuel types can be analyzed by examining the linear, quadratic, and interaction impacts of corrosion factors. Fig. 4 depicts the steps involved in corrosion modeling using the RSM technique. Two sets of data are used to generate an output: fuel type (B0–B20)/(WFOB0-WFO20) and exposure time (240–720 h). This section involves the choice of optimum corrosion conditions for minimizing the corrosivity of fuel types susceptible to Br and Cu. The RSM was used to perform independent variable optimization. The development of the RSM model takes into account not only the responses (CR_{Cu} and CR_{Br}), but also a number of independent variables (fuel kinds and exposure length. The CCD approach was used to evaluate the impact of fuel types and exposure duration on the CRs of Cu and Br in this investigation.

2.4.2. Development ANFIS model

The corrosion rates of Cu and Br in the WSOB/diesel blend environment were predicted in this work using ANFIS.With training data, a Sugeno fuzzy system was created using the program Matlab R2014a and the fuzzy logic toolbox for each trial. Table 3 highlights the development of Mamdani based fuzzy model for the prediction of corrosion rate of Cu and Br with respect to the variation of blends and exposure duration. The input parameters were assigned with three membership functions (MFs) such as Low, Medium and High and subsequently the responses discretised in to nine MFs like VVL, VL, ML, L, M, H, MH, VH, VVH [27]. Table 4 summarizes the fuzzy rules developed based on the experimental data. The MFs have nine set of rules with and gate for predicting the corrosion rate of Cu and Br which is illustrated in Table A1 (See Appendix 3).

The approach for fuzzy modelling is shown in Fig. 5. As seen, database/fuzzification meticulously evaluates each input value before converting it into linguistic terms. For this linguistic terms assignment, we obtain fuzzy MF values between 0 and 1 [28]. There are numerous different mf kinds; for this study, a triangular mf is chosen. The rule base has carried out the interference operation on the

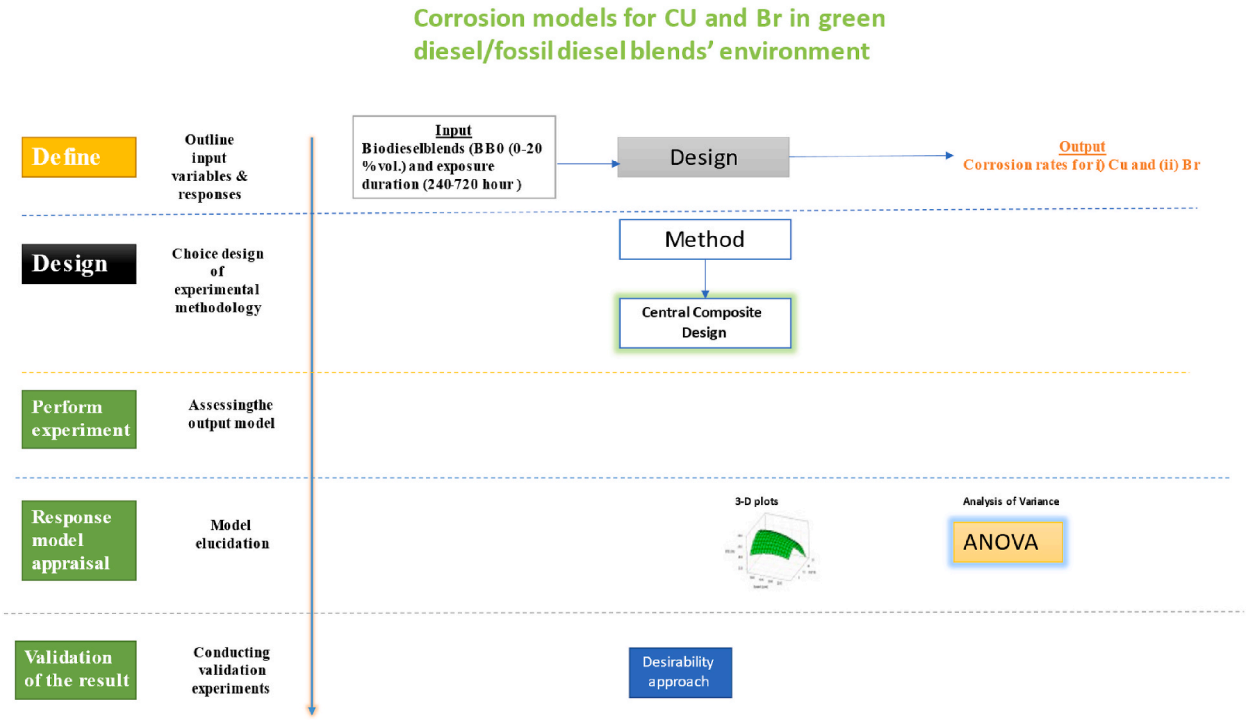

Fig. 4. Graphic flow for the empirical based modelling.

Table 3
Fuzzy linguistic variables and range of corrosion parameters.

Input			
Linguistic variables	Range of Blends (v/v%)	Linguistic variables	Range of Exposure duration (hours)
Low	0	Low	240
Medium	10	Medium	480
High	20	High	720
Response			
Linguistic variables	**Range of Corrosion rates of Cu (mpy)**	**Linguistic variables**	**Range of Corrosion rates of Br (mpy)**
VVL	0.017–0.042	VVL	0.010–0.030
ML	0.042–0.067	ML	0.030–0.049
M	0.067–0.092	M	0.049–0.068
VVL	0.092–0.117	VVL	0.068–0.087
L	0.117–0.143	L	0.087–0.107
H	0.143–0.168	H	0.107–0.126
VVL	0.168–0.193	VVL	0.126–0.145
M	0.193–0.218	VVL	0.145–0.165
VVH	0.218–0.243	VVH	0.165–0.184

L = Low, M = medium, H = high, VVL = very very low, VVH = very very high.

Table 4
Fuzzy rules.

Blends (v/v%)	Exposure duration (hours)	Corrosion rates of Cu (mpy)	Corrosion rates of Br (mpy)
Low	Low	VVL	VVL
Low	Medium	ML	ML
Low	High	M	M
Medium	Low	VVL	VVL
Medium	Medium	L	L
Medium	High	H	H
High	Low	VVL	VVL
High	Medium	M	VVL
High	High	VVH	VVH

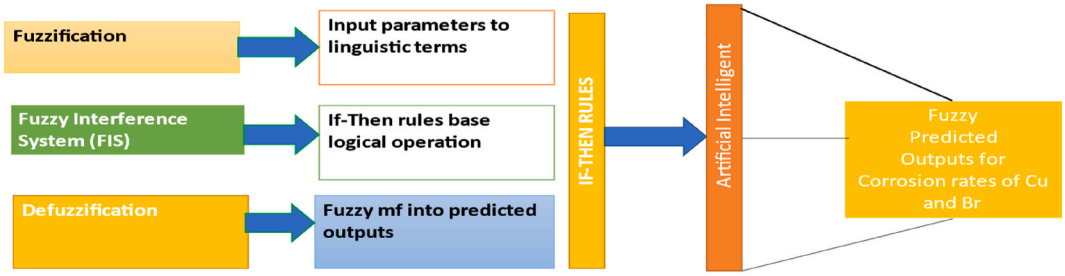

Fig. 5. Schematic diagram for fuzzy theory process.

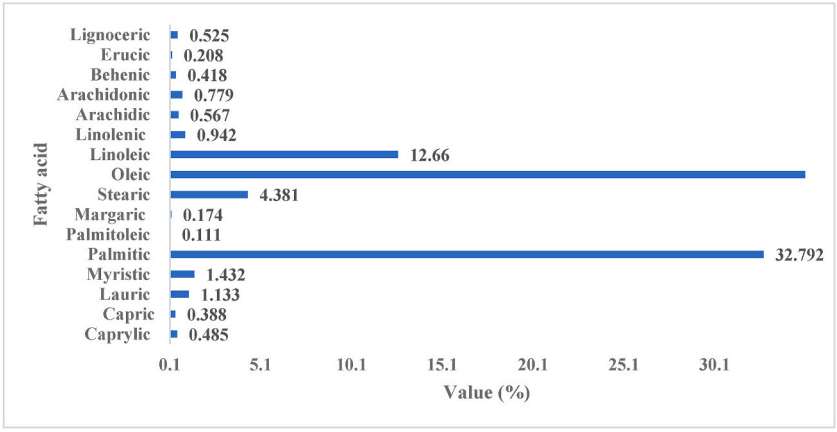

Fig. 6. Fatty acid content of WFOB.

rules. Fuzzy interference is made up of logical operation, IF-THEN rules, and MF. It considered the relationship between the input-output data in accordance with their linguistic forms [29]. The Mamdani model is recommended in this study among other rule-based systems. The final stage in the fuzzy development process is defuzzification. It involves a method for transforming mf into a choice.

2.4.3. *Determination of Statistical indices for the RSM and ANFIS models*

Statistical features viz. The correlation coefficient (R), the regression coefficient (R^2), the root mean square error (RMSE), the mean average error (MAE), the standard error of prediction (SEP), and the absolute standard deviation (ASD) were adopted to judge the effectiveness of the hybrid models and their ability to predict outcomes. Statistics for both the RSM and ANN models were estimated using Eqs. (7)–(12).

$$R = \left(\frac{\sum_{m=1}^{n} \left(T_{pre,m} - T_{pred}\right)\left(T_{exp.m} - T_{exp}\right)}{\sqrt{\sum_{m=1}^{n} \left(T_{pre.m} - T_{pred}\right)^2 \sum_{m=1}^{n} \left(T_{exp.m} - T_{exp}\right)^2}} \right) \tag{7}$$

$$R^2 = 1 - \frac{\sum_{i=1}^{n} \left(T_{i,p} - T_{1,e}\right)^2}{\sum_{i=1}^{n} \left(T_{i,p} - T_{e,ave}\right)^2} \tag{8}$$

$$\mathrm{MSE} = \sqrt{\frac{\sum_{i=1}^{n} \left(\mathrm{T_{i,e}} - \mathrm{T_{i,p}}\right)^2}{\mathrm{n}}} \tag{9}$$

$$\mathrm{MAE} = \sum_{i=1}^{n} \frac{\left|\left(\mathrm{T_{i,e}} - \mathrm{T_{i,p}}\right)\right|}{\mathrm{n}} \tag{10}$$

Table 5
Properties of fuel for corrosion study.

	Types of fuel				
Fuel properties	B0	B10	B20	B100	EN 41214
Density (kg/m^2)	861.3	862.6	865.3	883.6	850–900
Viscosity (mm^2/s) @ 40 °C	4.7162	4.7614	4.8910	5.1282	3.5–5.0
Flash point (°C)	72	74	78	142	120 min
Acid value (mg KOH/g)	0.12	0.14	0.17	0.298	0.50 max

Table 6
Design matrix for the corrosion of copper and brass.

Coded process variables		Experimental data		Predicted data by RSM	
Blends (v/v %)	Exposure duration (hours)	Corrosion rates of Cu (mpy)	Corrosion rates of Br (mpy)	Corrosion rates of Cu (mpy)	Corrosion rates of Br (mpy)
−1	−1	0.0173	0.011	0.0204	0.006
+1	−1	0.0254	0.0215	0.0238	0.017
0	+1	0.1196	0.106	0.1113	0.124
+1	+1	0.2429	0.184	0.2299	0.136
−1	0	0.0753	0.0639	0.0659	0.065
+1	0	0.1268	0.0102	0.1268	0.077
0	−1	0.017	0.0109	0.0221	0.012
0	+1	0.1427	0.109	0.1706	0.13
0	0	0.0971	0.0807	0.0963	0.071
0	0	0.0971	0.0807	0.0963	0.071
0	0	0.0971	0.0807	0.0963	0.071
0	0	0.0971	0.0807	0.0963	0.071
0	0	0.0971	0.0807	0.0963	0.071

Table 7a
ANOVA for the CR of Cu in WFOB.

Source	Sum of Squares	Df	Mean Square	F-value	p-value	
Model	0.1257	5	0.0251	264.28	<0.0001	*SIGN
A-Blend	0.011	1	0.011	115.35	<0.0001	SIG
B-Exposure duration	0.1054	1	0.1054	1108.16	<0.0001	SIG
AB	0.0036	1	0.0036	37.34	0.0005	SIG
A^2	0.0007	1	0.0007	7.03	0.0329	**NSIG
B^2	0.0057	1	0.0057	60.45	0.0001	SIG
Residual	0.0007	7	0.0001			
Lack of Fit	0.0007	3	0.0002			
Pure Error	0	4	0			
Cor Total	0.1263	12				

*Significant; **Non-significant.

$$SEP = \frac{RMSE}{T_{e,ave}} \tag{11}$$

$$AD = \frac{100}{n}\sum_{i=1}^{n}\frac{\left|\left(T_{i,e} - T_{i,p}\right)\right|}{\left(T_{i,e}\right)} \tag{12}$$

3. Results and discussion

3.1. WFOB's fatty acid contents and fuel physicochemical features

Fig. 6 displays the fatty acid composition.The weight of WFOB is composed of 84.6% saturated and 15.4% unsaturated fatty acid compositions. Samuel et al. [30] stated that saturated fatty acid in WFOB can both raise cetane number and increase NOx. To be regarded as commercially sustainable, the developed biodiesel must satisfy the certification requirements of the EN 14214 specification. The characteristics of the various fuels are listed in Table 5. The key parts were discovered to comply with European requirements.The diesel engine does not require modification because the fuel types have not changed appreciably [31].

Table 7b
ANOVA for the CR of Br in WFOB.

Source	Sum of Squares	Df	Mean Square	F-value	p-value	
Model	0.0213	2	0.0106	13.23	0.0016	SIG
A-Blend	0.0002	1	0.0002	0.2510	0.6272	NSIG*
B-Exposure duration	0.9211	1	0.0211	26.21	0.00025	SIG**
Residual	0.0080	10	0.0008			
Lack of Fit	0.0080	6	0.0013			
Pure Error	0.0000	4	0.0000			
Cor Total	0.0293	12				

*Significant; **Non-significant.

3.2. Modelling and extrapolative fitness of RSM and ANOVA CRs

Table 6 highlights the design layout for the corrosion examination of copper and brass in WFOB. As detected, the highest CRs of copper (0.2429 mpy) and brass (0.1840 mpy) were attained at a blend ratio of 20% and exposure duration of 720 h while the minimum CRs of copper (0.0173 mpy) and brass (0.0110 mpy) were reached at a blend ratio of unblended diesel (B0) and exposure duration of 240 h.

Tables (7a) and (7b) are the groupings of Table 7: The ANOVA for the CRs of Cu and Br exposed to WFOB is summarized in Tables (7a) and (7b), respectively.. As seen in Table 7a, the model F-value of 264.28 implies that the model is substantial. Due to an extremely low probability of only 0.01%, this high F-value cannot be explained by chance alone. When the probability of a term in the

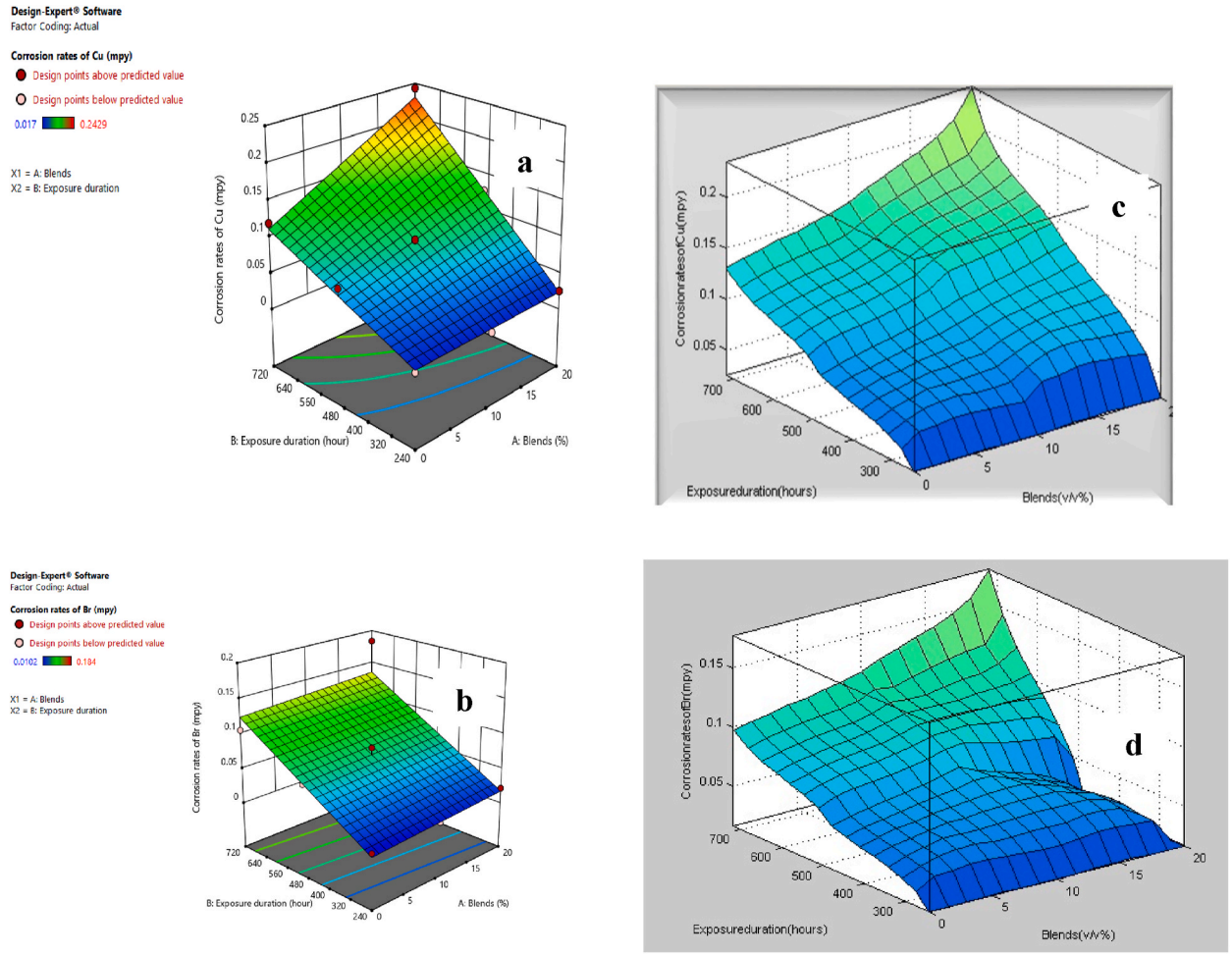

Fig. 7. Three-dimensional surface plots by RSM (a) Copper corrosion rates (CRs) in relation to fuel types and exposure durations (b) Brass CRs in relation to fuel types and exposure durations; and ANFIS curves: (c) Copper CRs in relation to fuel types and exposure duration, and (d) Brass CRs in relation to fuel types and exposure duration.

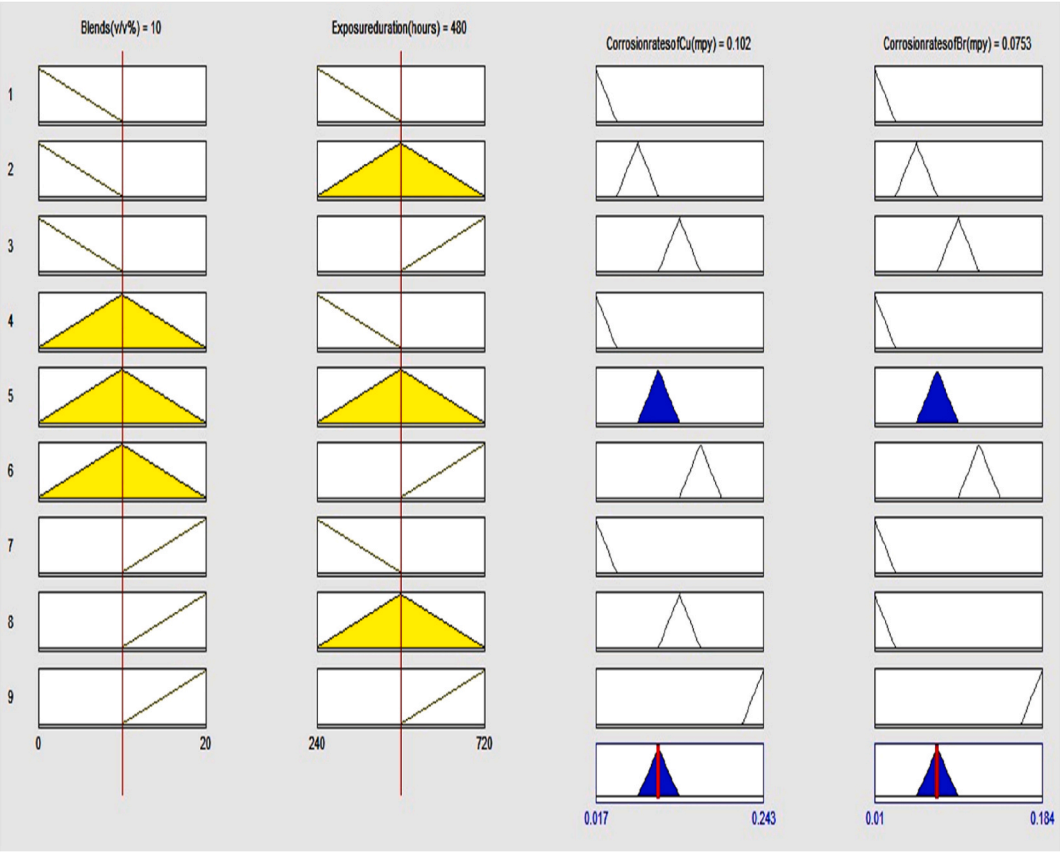

Fig. 8. Fuzzy rule viewer.

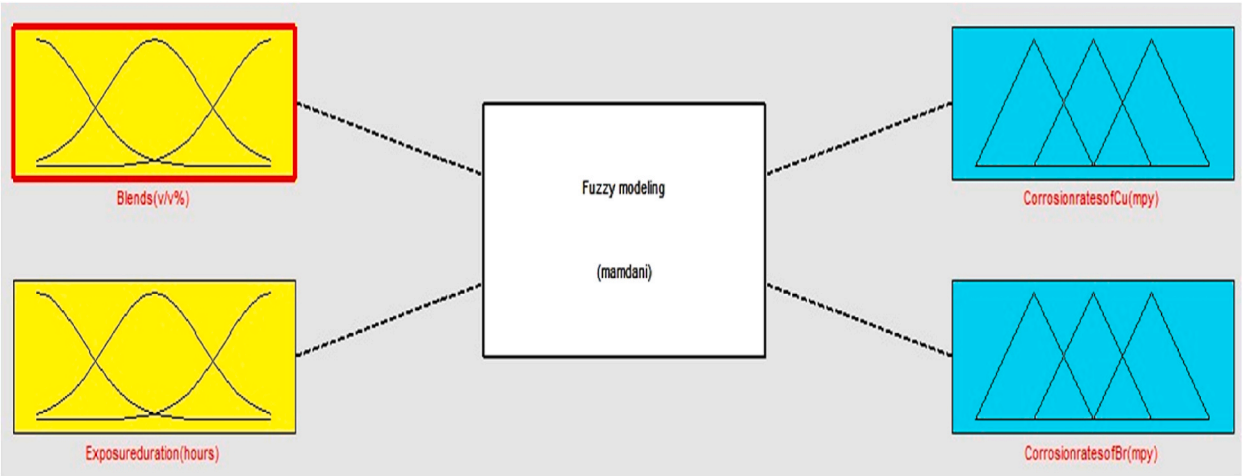

Fig. 9. Established fuzzy interference system.

model is smaller than 0.0500, we say that it is noteworthy. In this case, the quadratic terms of fuel type (A^2) and exposure duration (B^2) are as important as the linear terms of fuel type (A). However, other factors are not momentous. For instance, if the number is higher than 0.1000, it means that the model terms are not important. Model reduction can be useful if your model has a large number of irrelevant terms (excluding those necessary to maintain hierarchy). The model F-value of 13.23, as shown in Table 7b, also indicates the model's significance. It's not as close as one may assume between the "Pred R-Squared" value of 0.4266 and the "Adj R-Squared" value of 0.6709. This could indicate possible problems with your model and/or data, such as model simplification, data translation,

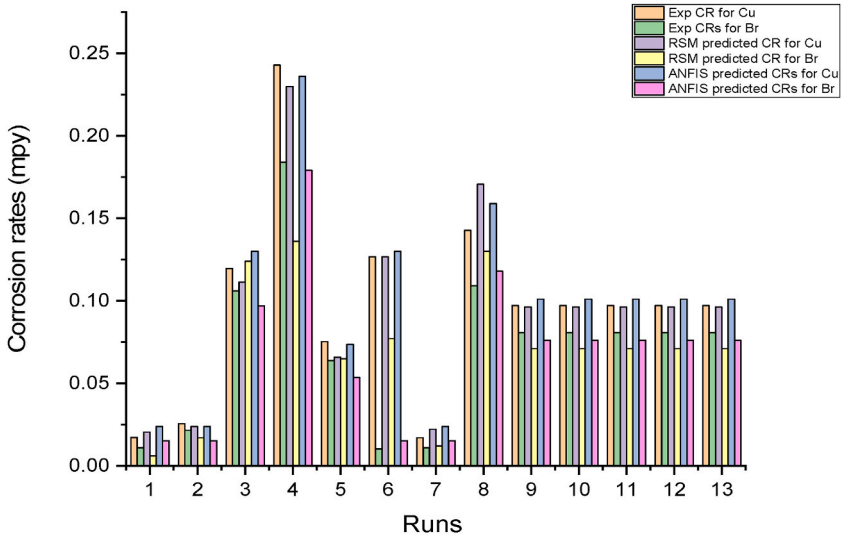

Fig. 10. Runs vs. Experimental, RSM, and ANFIS predicted corrosion rates.

outlier detection, etc. The "Adeq Precision" metric assesses the quality of the signal over the background noise. Ratios greater than 4 are preferred. A signal strength of 9.554 shows sufficient ratio. Using this model, you may further explore potential layout options.

The response surface model obtained to check the corrosion rate of Cu in WFOB including all experimental variables is signified by Eq. (13a) in terms of coded experimental variables and Eq. (13b) in terms of actual experimental variables. Eq. (14a) epitomizes the response surface model obtained to check the corrosion rate of brass in WFOB in terms of coded experimental variables, while Eq. (14b) signifies the model in terms of real experimental data.

$$CR_{Cu} = 0.096 + 0.030A + 0.074B + 0.029AB \tag{13a}$$

$$\mathrm{CR_{Cu}} = -0.025037 - 0.002712\mathrm{Blend} + 0.0001894\mathrm{Exposure\ duration} + 0.012 + 0.029\mathrm{Fuel\ blend} * \mathrm{Exposure\ duration} \tag{13b}$$

$$\mathrm{CR_{Br}} = 0.071 + 0.0058\mathrm{A} + 0.0\mathrm{B} + 0.059\mathrm{AB} \tag{14a}$$

$$\mathrm{CR_{Br}} = -0.053564 + 0.00058\mathrm{Blend} + 0.000247\mathrm{Exposure\ duration} \tag{14b}$$

3.3. RSM model, fuzzy model forecast and its defuzzification

The three-dimensional surface plots by RSM for copper corrosion rates (CRs) versus fuel types and exposure durations, as well as brass CRs versus fuel types and exposure durations, are shown in Fig. 7(a and b). Fig. 7(c and d) shows the three-dimensional surface plots produced by ANFIS curves for copper and brass CRs in relation to fuel types and exposure times, respectively. The discrepancies in the phenomenon associated with the CRs' parameters vs. CRs of Cu and Br discussed elsewhere [18]. The CRs became exceedingly aggravated at a higher WFOB and exposure duration [32].

Using the fuzzy model, the last layer of the fuzzy system generates the predicted rates of Cu and Br corrosion.The defuzzifier model is shown in Fig. 8. As demonstrated, the control variables of 10% WSOB blends and 480 h of exposure led to the comparable fuzzy model projected values of CRs for Cu (0.102 mpy) and Br (0.0753 mpy).The uniformly distributed data sets for corrosion rates indicate that the fuzzed forecasted CRs of Cu and Br are close to those of the experimental values [33–35] (see Fig. 9).

3.3.1. ANFIS based modelling of corrosion

Fig. 8 shows the architecture of the developed ANFIS model, which includes two inputs (fuel kinds and exposure duration) and two outputs (responses) (corrosion rates of Cu and Br). As oberved, fuzzy systems with 9 inference rules and three Gaussian membership functions for each entering input were sufficient to represent process performance.

3.4. Comparing of RSM and ANFIS models

Fig. 10 depicts the experimental CRs for Cu and Br, as well as those of the RSM-ANFIS models. When compared to the models derived from the RSM on various runs, the CRs model from the ANFIS is extremely near to the experimental CRs, as shown. Other researchers have reported similar findings [36,37].

Fig. 11(a and b) compares experimental and RSM predicted CRs for Cu and Br, whereas Fig. 11(c and d) contrasts experimental and ANFIS predicted CRs for Cu and Br. The linear equations $(0.9734x + 0.0026)$ and $(0.7244x + 0.0197)$ are discovered to be adequate for

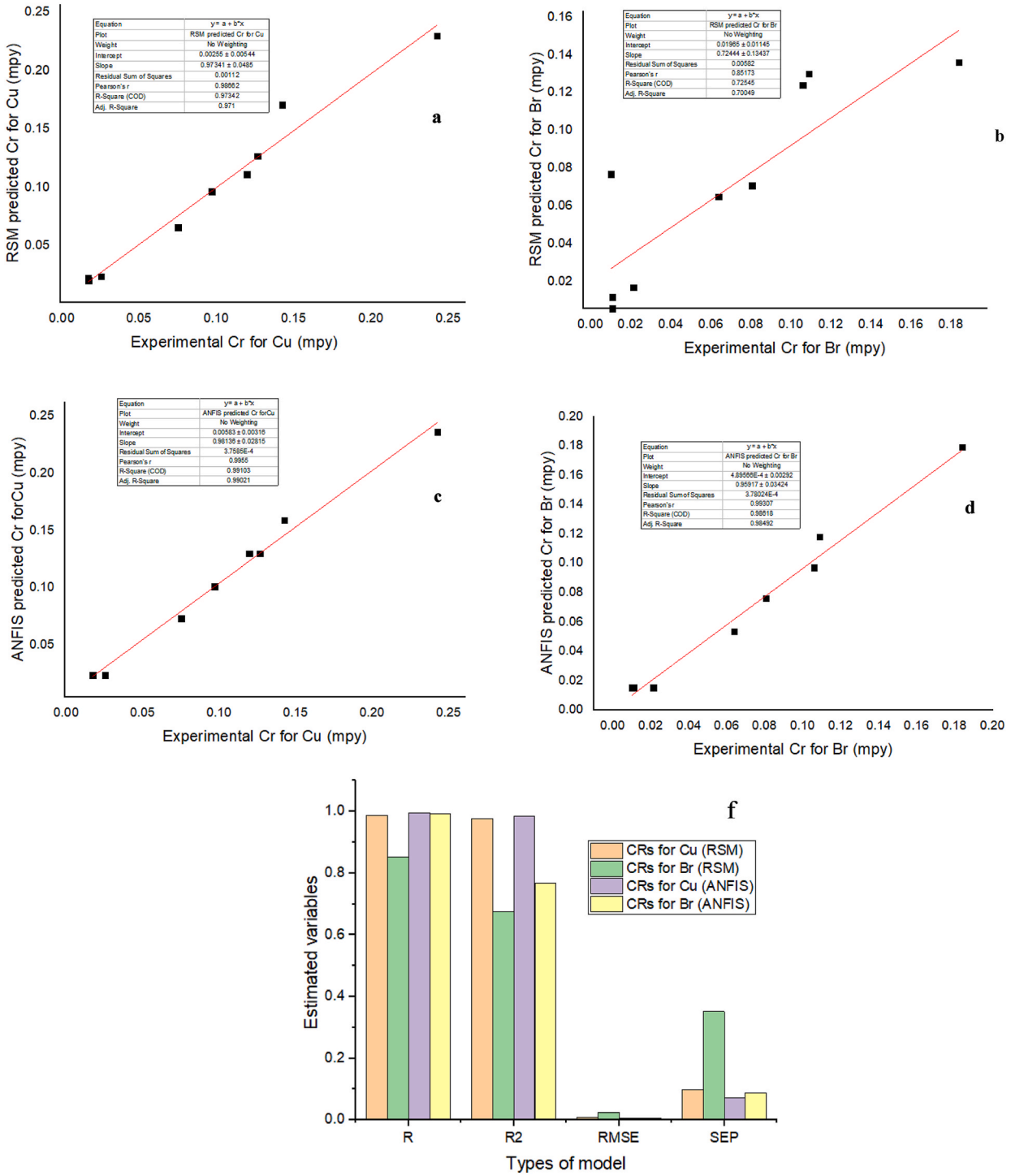

Fig. 11. Contrast of the various corrosion rates: (a) RSM predicted and experimental CRs for Cu, (b) RSM predicted and experimental CRs for Br, (c) ANFIS predicted and experimental CRs for Cu, and (d) ANFIS predicted and experimental CRs for Br. f. Catalogues of RSM and ANFIS models.

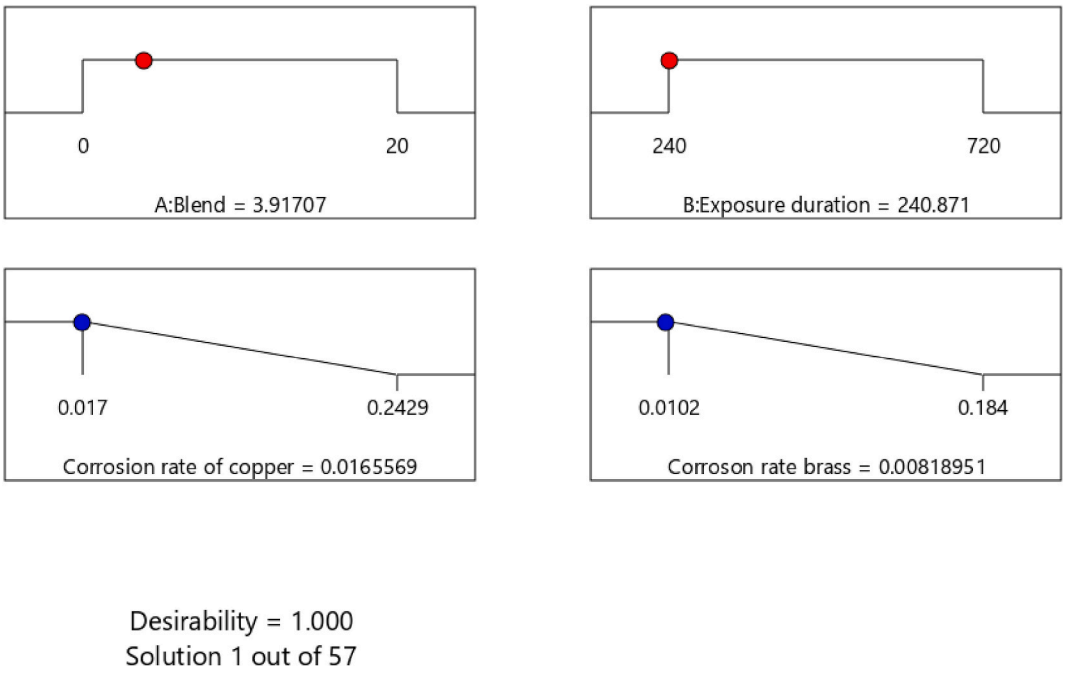

Fig. 12. Optimal condition for corrosion minimization for Cu and Br in biodiesel environment.

Table 8
Mechanical properties of corroded Cu and Br.

AP[a]	Hardness number (N/mm^2)	Tensile strength (MPa)
Cu	211.12	717.80
Br	68.63	1476.52

[a] Automotive parts.

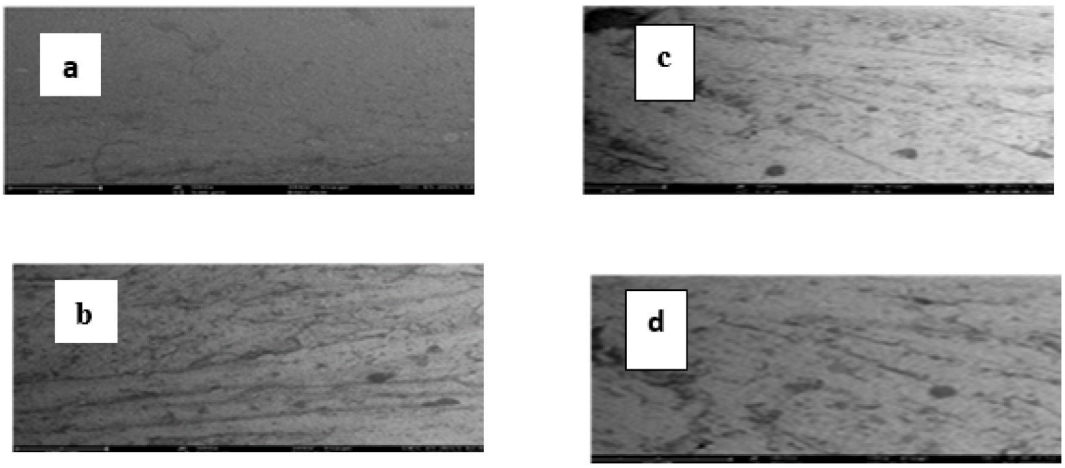

Fig. 13. SEM Morphologies of Cu and Br: (a) Cu before exposure, (b) Cu after exposure, (c) Br before exposure, (d) Br after exposure.

the variations of experimental and RSM-based CRs, respectively, whereas the rectilinear equations $(0.981x+0.00583)$ and $(0.9592x+0.000489)$ are also found to be appropriate for these same variations for copper and brass, respectively. The RSM had an R^2 of 0.7254 and 0.9734 for the CRs of brass and copper, while the ANFIS had an R^2 of 0.98618 and 0.99103, indicating that the ANFIS model captured a greater proportion of the data than the RSM model. As a result, the ANFIS model could predict CRs for brass and copper in a biodiesel environment. Analogous reports were stated by researchers elsewhere [16,38,39]. To get precise predictions of

the Cu and Br CRs in a biodiesel environment, it is vital to contrast the superiority of RSM and ANFIS. In this study's comparison of prediction power between the RSM and ANFIS models, a few statistical norms were used (See Fig. 11(f)).

3.5. Corrosions' optimal condition for minimization and its mechanical properties

Fig. 12 shows the optimal conditions for lessening Cu and Br CRs in a biodiesel environment. The CRs of Cu (0.01656 mpy) and Br (0.008189) were detected to be optimal at B 3.91 of biodiesel/diesel blend and exposure duration of 240.9 h. In a validation test, optimized experimental variables resulted in experimental CRs of 0.01655 mpy and 0.0081895 mpy for Cu and Br, respectively. Comparing projected and measured of CRs for Cu and Br, the average error was 0.06% and 0.03054%, respectively. Good agreement between the percentages of error in prediction was found during validation, proving that the RSM model developed was reliable. Table 8 highlights the mechanical properties of Cu and Br exposed to biodiesel at optimal conditions, namely HAN and TES. As can be realized, the TES of Br was higher than copper while the hardness of the latter exceeded that of the former. The increased oxygen dissociation and stronger conductivity of the optimal corroded biodiesel of Br to Cu are the reason of the higher hardness number and tensile strength [32].

3.6. Surface morphology of the automotive parts

Under optimal conditions, Fig. 13(a and b) shows the SEM morphologies of Cu before and after exposure, while Fig. 13(c and d) shows the SEM morphologies of Br before and after exposure. The microstructure of copper darkens in comparison to brass. Brass is more computably more than copper, which explains this phenomena.

4. Conclusion

The study demonstrated the prediction and modelling of copper and brass CRs in biodiesel synthesized using RSM and ANFIS models. The best conditions and correlations for predicting and modelling the CRs of these automotive parts were recognized. The mechanical properties of automotive parts, specifically HAN and TES, as well as surface morphologies prior to exposure and under optimal conditions, were examined. To attain a vigorous study in the nearby imminent, (i) additional operating corrosion variables can be studied, (ii) the inclusion and efficacy of cost-effective inhibitors can be studied, and (iii) kinetic and thermodynamic features can be studied further. The following conclusions can be deduced from this study:

- The optimum CRs for copper and brass were 0.01656 mpy and 0.008189 mpy at a B 3.91 biodiesel/diesel blend and 240.9-h exposure.
- The developed ANFIS model outperformed the RSM model in terms of application and superiority.
- When compared to the RSM model, the ANFIS model had a higher coefficient of determination and lower values of root mean squared errors (RMSE), mean average error (MAE), and average absolute deviation (AAD); this validates the ANFIS model's superiority for predicting copper and brass CRs.
- Brass had a higher tensile strength than copper, although the latter had a higher hardness number.

CRediT authorship contribution statement

Olusegun David Samuel: Writing – original draft, Methodology, Investigation, Formal analysis, Data curation, Conceptualization. **Modestus O. Okwu:** Writing – review & editing, Validation, Methodology. **Varatharajulu Muthukrishnan:** Writing – review & editing, Visualization, Methodology. **Ivrogbo Daniel Eseoghene:** Writing – review & editing, Visualization. **H. Fayaz:** Writing – review & editing, Investigation.

Declaration of competing interest

The authors declare the following financial interests/personal relationships which may be considered as potential competing interests:Attached please find our new manuscript entitled "Adaptive neuro-fuzzy inference system for forecasting corrosion rates of automotive parts in biodiesel environment" co-authored by Olusegun David Samuel, Modestus O. Okwu, Varatharajulu Muthukrishnan, Ivrogbo Daniel Eseoghene, H. Fayaz.

Acknowledgments

For the use of their JCM 100 small scanning electron microscope, the authors would like to thank the Chemical Engineering Department at Ahmadu Bello University.

Appendix 1. The vessel employed for keeping fuel types

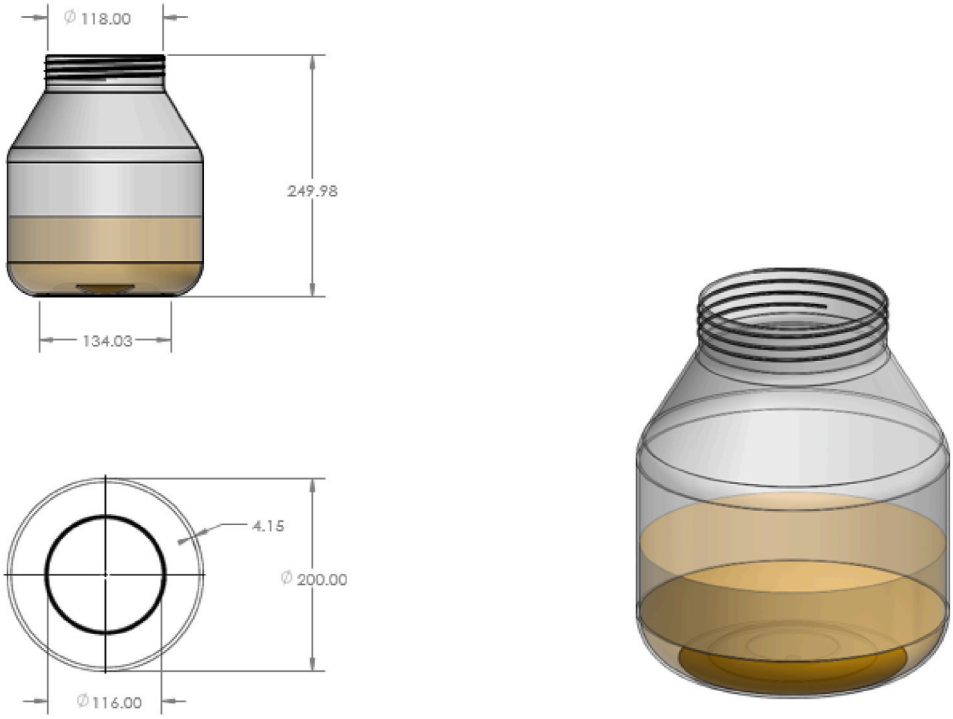

Fig. 1A. The dimension of the vessel employed for keeping fuel types.

Appendix 2. The apparatus adopted in corrosion testing

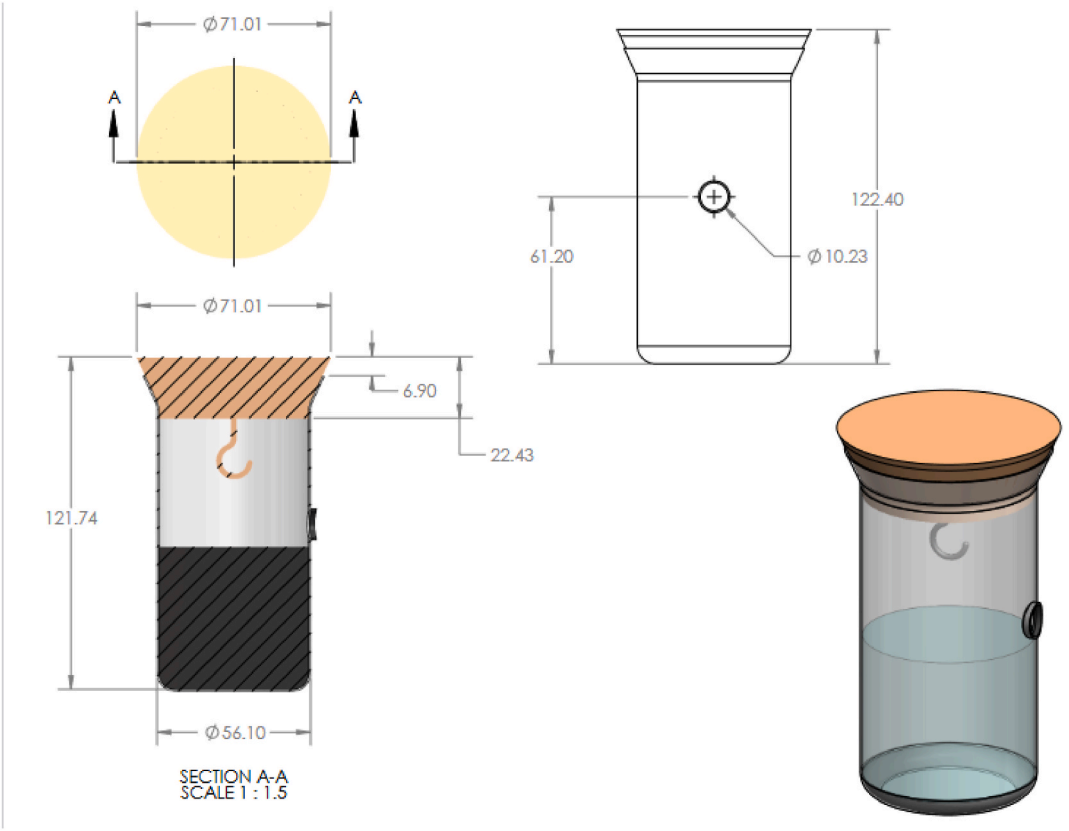

Fig. 2A. The dimension of apparatus adopted in corrosion testing.

Appendix 3. Expanded View of Fuzzy Rules

Table A1
Fuzzy rules

S/N	Set of rules
i.	For low blend and low exposure duration then CR of Cu is VVL and CR of Br is VVL
ii	For low blend and medium exposure duration then CR of Cu is ML and CR of Br is ML
iii.	For low blend and high exposure duration then CR of Cu is M and CR of Br is M
iv.	For medium blend and low exposure duration then CR of Cu is VVL and CR of Br is VVL
v.	For medium blend and medium exposure duration then CR of Cu is L and CR of Br is L
vi	For medium blend and high exposure duration then CR of Cu is H and CR of Br is H.
vii	For high blend and low exposure duration then CR of Cu is VVL and CR of Br is VVL
viii	For high blend and medium exposure duration then CR of Cu is M and CR of Br is VVL
ix	For high blend and high exposure duration then CR of Cu is VVH and CR of Br is VVH

L = Low; M = medium; H = high; VVL = very very low; VVH = very very high; ML = medium low; CR = corrosion rate.

References

[1] S. Oyedepo, Energy and sustainable development in Nigeria: the way forward, Energy, Sustainability and Society 2 (1) (2012) 1–17.
[2] O. Samuel, M. Gulum, Mechanical and corrosion properties of brass exposed to waste sunflower oil biodiesel-diesel fuel blends, Chem. Eng. Commun. 206 (5) (2019) 682–694.
[3] O. Samuel, M. Kaveh, O. Oyejide, P. Elumalai, T. Verma, K. Nisar, C. Saleel, A. Afzal, O. Fayomi, H. Owamah, S. Sarıkoç, Performance comparison of empirical model and Particle Swarm Optimization & its boiling point prediction models for waste sunflower oil biodiesel, Case Stud. Therm. Eng. 33 (2022) 101947.

[4] O. Samuel, M. Waheed, A. Taheri-Garavand, T. Verma, O. Dairo, B. Bolaji, A. Afzal, Prandtl number of optimum biodiesel from food industrial waste oil and diesel fuel blend for diesel engine, Fuel 285 (2021) 119049.
[5] R. Estevez, L. Aguado-Deblas, F. López-Tenllado, C. Luna, J. Calero, A. Romero, F. Bautista, D. Luna, Biodiesel is dead: long life to advanced biofuels—a comprehensive critical review, Energies 15 (2022) 3173.
[6] M. Jakeria, M. Fazal, A. Haseeb, Influence of different factors on the stability of biodiesel: a review, Renew. Sustain. Energy Rev. 30 (2014) 154–163.
[7] B. Singh, J. Korstad, Y. Sharma, A critical review on corrosion of compression ignition (CI) engine parts by biodiesel and biodiesel blends and its inhibition, Renew. Sustain. Energy Rev. 16 (5) (2012) 3401–3408.
[8] S. Thangavelu, A. Ahmed, F. Ani, Impact of metals on corrosive behavior of biodiesel-diesel-ethanol (BDE) alternative fuel, Renew. Energy 94 (2016) 1–9.
[9] M. Fazal, A. Haseeb, H. Masjuki, Degradation of automotive materials in palm biodiesel, Energy 40 (1) (2012) 76–83.
[10] M.A.A. Parameswaran, S. Krishnamurthy, A comparison of corrosion behaviour of copper and its alloy in Pongamia pinnata oil at different conditions, J. Energy (2013) 1–4.
[11] C. Akhabue, F. Aisien, C. Ojo, The effect of Jatropha oil biodiesel on the corrosion rates of aluminium and mild carbon steel, Biofuels 5 (5) (2014) 545–550.
[12] B. Oni, S. Sanni, B. Ezurike, E. Okoro, Effect of corrosion rates of preheated Schinzochytrium sp. microalgae biodiesel on metallic components of a diesel engine, Alex. Eng. J. 61 (10) (2022) 7509–7528.
[13] P. Sharma, M. Sivaramakrishnaiah, B. Deepanraj, R. Saravanan, M. Reddy, A novel optimization approach for biohydrogen production using algal biomass, Int. J. Hydrogen Energy (2022), https://doi.org/10.1016/j.ijhydene.2022.09.274.
[14] Z. Said, P. Sharma, Q. Nhuong, B. Bora, E. Lichtfouse, H. Khalid, R. Luque, X. Nguyen, A. Hoang, Intelligent Approaches for Sustainable Management and Valorisation of Food Waste, Bioresource Technology., 2023 128952, https://doi.org/10.1016/j.biortech.2023.128952.
[15] A. Jain, B. Bora, R. Kumar, P. Sharma, H. Deka, Theoretical potential estimation and multi-objective optimization of Water Hyacinth (Eichhornia Crassipes) biodiesel powered diesel engine at variable injection timings, Renew. Energy 206 (2023) 514–530.
[16] L. Emembolu, P. Ohale, C. Onu, N. Ohale, Comparison of RSM and ANFIS modeling techniques in corrosion inhibition studies of Aspilia Africana leaf extract on mild steel and aluminium metal in acidic medium, Applied Surface Science Advances 11 (2022) 100316.
[17] O. Samuel, M. Okwu, Comparison of Response Surface Methodology (RSM) and Artificial Neural Network (ANN) in modelling of waste coconut oil ethyl esters production, Energy Sources, Part A Recovery, Util. Environ. Eff. 41 (9) (2019) 1049–1061.
[18] A. Shehzad, A. Arslan, F. Rehman, M. Quazi, S. Butt, M. Jamshaid, Corrosion behavior of copper, aluminium, and stainless steel 316L in chicken fat oil based biodiesel-diesel blends, Sustain. Energy Technol. Assessments 56 (2023) 103098.
[19] M. Aghaaminiha, R. Mehrani, M. Colahan, B. Brown, M. Singer, S. Nesic, S. Vargas, S. Sharma, Machine learning modeling of time-dependent corrosion rates of carbon steel in presence of corrosion inhibitors, Corrosion Sci. 193 (2021) 109904.
[20] Q. Hu, Y. Liu, T. Zhang, S. Geng, F. Wang, Modeling the corrosion behavior of Ni-Cr-Mo-V high strength steel in the simulated deep sea environments using design of experiment and artificial neural network, J. Mater. Sci. Technol. 35 (1) (2019) 168–175.
[21] R. Tuntas, B. Dikici, An ANFIS model to prediction of corrosion resistance of coated implant materials, Neural Comput. Appl. 28 (2017) 3617–3627.
[22] O. Nkuzinna, M. Menkiti, O. Onukwuli, G. Mbah, B. Okolo, M. Egbujor, Application of Factorial Design of Experiment for Optimization of Inhibition Effect of Acid Extract of Gnetum Africana on Copper Corrosion, Natural resources., 2014.
[23] K. Goh, T. Lim, P. Chui, Evaluation of the effect of dosage, pH and contact time on high-dose phosphate inhibition for copper corrosion control using response surface methodology (RSM), Corrosion Sci. 50 (4) (2008) 918–927.
[24] I.P. Aquino, R.P.B. Hernandez, D.L. Chicoma, H.P.F. Pinto, I.V. Aoki, Influence of light, temperature and metallic ions on biodiesel degradation and corrosiveness to copper and brass, Fuel 102 (2012) 795–807.
[25] A. S. T. M, Standard, "Standard Practice for Preparing, Cleaning, and Evaluating Corrosion Test Specimens, American Society for Testing and Materials G1-03, 2011.
[26] J. Holman, Experimental Methods for Engineers, McGraw-Hill, 2012.
[27] B. Paramasivam, S. Kumanan, V. Kavimani, M. Varatharajulu, Fuzzy-based prediction of compression ignition engine distinctiveness powered by novel graphene oxide nanosheet additive diesel–Aegle marmelos pyrolysis oil ternary opus, International Journal of Energy and Environmental Engineering (2022) 1–19.
[28] A. Karkevandi-Talkhooncheh, S. Hajirezaie, A. Hemmati-Sarapardeh, M. Husein, K. Karan, M. Sharifi, Application of adaptive neuro fuzzy interface system optimized with evolutionary algorithms for modeling CO2-crude oil minimum miscibility pressure, Fuel 205 (2017) 34–45.
[29] D. Bhowmik, P. Gaur, Optimal placement of capacitor banks for power loss minimization in transmission systems using fuzzy logic, J. Eng. Sci. Technol. 13 (10) (2018) 3190–3203.
[30] O. Samuel, M. Kaveh, T. Verma, A. Okewale, S. Oyedepo, F. Abam, C. Nwaokocha, M. Abbas, C. Enweremadu, E. Khalife, M. Szymanek, J. Dziwulski, C. Saleel, Grey Wolf Optimizer for enhancing Nicotiana Tabacum L. oil methyl ester and prediction model for calorific values, Case Stud. Therm. Eng. 35 (2022) 102095.
[31] O.D. Samuel, M.O. Okwu, S.T. Amosun, T.N. Verma, S.A. Afolalu, Production of fatty acid ethyl esters from rubber seed oil in hydrodynamic cavitation reactor: study of reaction parameters and some fuel properties, Ind. Crop. Prod. 141 (2019) 111658.
[32] D. Chandran, H.K. Ng, H.L.N. Lau, S. Gan, Y.M. Choo, Investigation of the effects of palm biodiesel dissolved oxygen and conductivity on metal corrosion and elastomer degradation under novel immersion method, Appl. Therm. Eng. 104 (2016) 294–308.
[33] A. Abdulshahed, A. Longstaff, S. Fletcher, The application of ANFIS prediction models for thermal error compensation on CNC machine tools, Appl. Soft Comput. 27 (2015) 158–168.
[34] B. Sen, U. Mandal, S. Mondal, Advancement of an intelligent system based on ANFIS for predicting machining performance parameters of Inconel 690–A perspective of metaheuristic approach, Measurement 109 (2017) 9–17.
[35] B. Paramasivam, Fuzzy prediction and RSM optimization of CI engine performance analysis: aegle marmelos non-edible seed cake pyrolysis oil as a diesel alternative, Energy Sources, Part A Recovery, Util. Environ. Eff. (2020) 1–17.
[36] M.İ. Coşkun, İ.H. Karahan, Modeling corrosion performance of the hydroxyapatite coated CoCrMo biomaterial alloys, J. Alloys Compd. 745 (2018) 840–848.
[37] T.I. Oguntade, C.S. Ita, O. Sanmi, D.T. Oyekunle, A binary mixture of sesame and castor oil as an ecofriendly corrosion inhibitor of mild steel in crude oil, Open Chem. Eng. J. 14 (1) (2020) 25–35.
[38] E. Betiku, V. Odude, N. Ishola, A. Bamimore, A. Osunleke, A. Okeleye, Predictive capability evaluation of RSM, ANFIS and ANN: a case of reduction of high free fatty acid of palm kernel oil via esterification process, Energy Convers. Manag. 124 (2016) 219–230.
[39] O. Samuel, J. Emajuwa, M. Kaveh, E. Emagbetere, F. Abam, P. Elumalai, C. Enweremadu, P. Reddy, I. Eseoghene, A. Mustafa, Neem-castor seed oil esterification modelling: comparison of RSM and ANFIS, Mater. Today Proc. (2023).